Difusion-Weighted MRI: from Brownian Motion to Head&Neck Tumor Characterization

C. Utrilla Contreras[1]*, B. Marín Aguilera[1], M. Buitrago Sánchez[1], J. Graessner[2] *, PS. García Raya[1]

[1]Department of Radiology, La Paz University Hospital, Madrid (Spain)
[2]Collaboration Management MR, Siemens Healthcare GmbH, Hamburg (Deutschland)

Received 17 August 2016 | Accepted 1 November 2016 | Published 23 December 2016

Abstract

This paper describes basic physics as well as clinical applications of diffusion-weighted magnetic resonance imaging. This is a technique that provides complementary information to conventional imaging sequences and it is applied in the field of oncologic imaging. This paper focuses on its specific application in head and neck, mainly in cancer patients, for characterization of primary tumors, and also for monitoring and predicting treatment response after chemotherapy or radiation therapy. Last, although diffusion-weighted imaging is shown to add value in several areas by being part of the multi-parametric magnetic resonance imaging approach, there are some unsolved challenges, which are proposed as future work.

Keywords

Diffusion-weighted Imaging, Magnetic Resonance Imaging, Oncologic Imaging, Tumor Characterization.

DOI: 10.9781/ijimai.2017.451

I. Introduction

Diffusion-weighted (DW) magnetic resonance (MR) imaging is a non-invasive functional MR imaging technique that provides complementary information for classic anatomical imaging sequences.

DW imaging is a form of MR imaging focuses on the micromovements (random, brownian) of the water molecules inside voxels. The relationship between histology and diffusion is complex, however generally densely cellular tissues or those with cellular swelling exhibit lower diffusion coefficients, and thus diffusion is particularly useful in tumor characterization and cerebral ischemia.

The diffusion characteristics of the tissue depend on its internal architecture (cellular packing, nucleus/cytoplasm ratio, intracellular organelles, cell membranes, nature of the extracellular matrix…) and its perfusion (micromotion of molecules in its capillaries) [1].

Molecular diffusion, or brownian motion, was first formally described by Einstein in 1905. Le Bihan *et al*. applied DWI on human brain for the first time in 1986 [2]. DW imaging has been used since the 1990s in central nervous system imaging, but recently the utilization of whole body DWI is becoming a standard application in routine imaging, more specifically, in the field of oncologic imaging.

II. Basics Physics

A. What is Diffusion?

Molecular diffusion is the random movement of molecules – in our case water (H_2O) – within tissues propelled by thermal energy. The motion of water protons in the extracellular compartment, the intravascular compartment, the interaction with cell membranes and intracellular water protons contribute to total diffusion.

The aim of these DW sequences is to obtain images whose contrast is influenced by the differences in water molecule mobility. Stejskal and Tanner [3] introduced the application of symmetric pair of pulsed gradients during the preparatory phase into the basic spin echo sequence that is T2 weighted.

B. How is MR Sensitizing the Tissue for Diffusion Effects?

Within the spin echo preparation period of an EPI sequence, two strong gradient pulses are played out around the 180° pulse. The first pulse dephases the magnetization of moving and static spins and the second pulse will not be able to completely undo the changes induced by the first gradient and rephases only static spins so that the signal experiments almost no changes. In contrast, moving water spins acquire non-zero phase dispersion, resulting in signal attenuation. Free water experiences the strongest signal attenuation at higher b-values (Fig. 1 & 2).

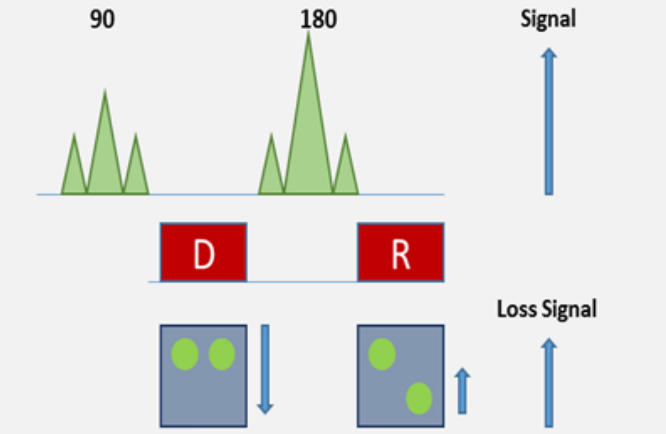

Fig. 1 a. Illustration of physical principles used for EPI diffusion-weighted imaging.

* Corresponding author.
E-mail addresses: cristinautrilla@hotmail.com (C. Utrilla Contreras), joachim.graessner@siemens.com (J. Graessner).

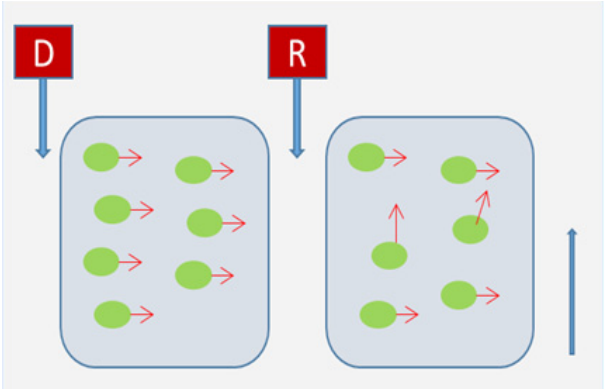

Fig. 1 b. Water molecules displace freely in all spatial directions, travelling long distances between the two gradient applications. These highly mobile molecules acquire phase information after the application of the first gradient, but due to their movement they don´t rephase completely after the application of the second gradient, losing signal.

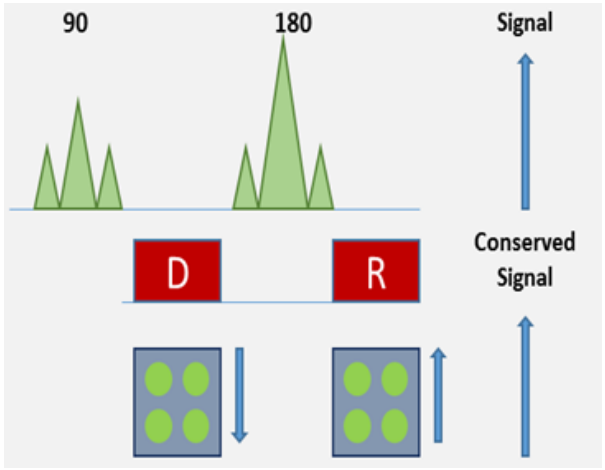

Fig 2. a. Illustration of physical principles used for EPI diffusion-weighted imaging.

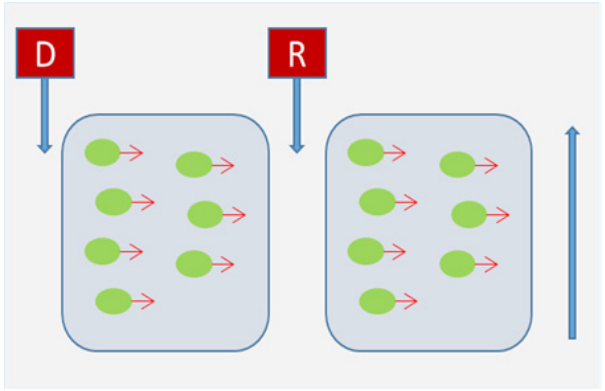

Fig. 2. b. Water molecules which are in a restricted environment don´t travel long distances so phase changes acquired during the application of the first gradient will be canceled by phase changes acquired during the second gradient, without losing signal.

C. What does the b-value Mean?

The degree of diffusion weighting of the sequence, expressed as the b-factor, depends on the characteristics of the diffusion gradients: gradient amplitude, application time and time between the two gradients.

The b-value identifies the measurements sensitivity to diffusion and determines the strength and duration of the diffusion gradients. It combines the following physical factors into b-values and is quantified by the apparent diffusion coefficient (ADC) measured in s/mm² (Fig. 3).

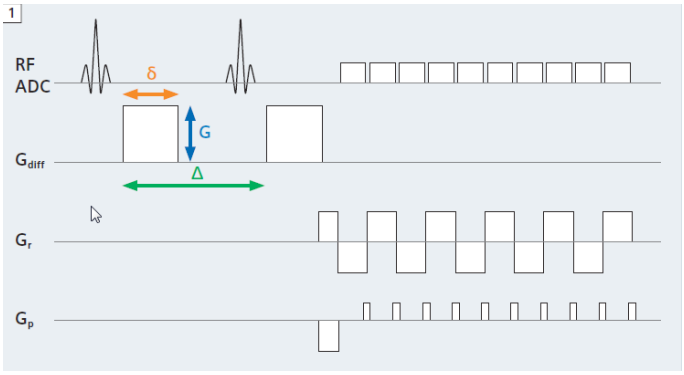

Fig. 3. Diagram of an EPI diffusion-weighted sequence illustrating the physical quantities of the b-values.

$$b = \gamma^2 G^2 \delta^2 (\Delta - \delta/3) \quad (1)$$

The signal ratio diffusion-weighted to non diffusion-weighted signal is:

$$\frac{S}{S_0} = e^{-\gamma^2 G^2 \delta^2 (\Delta - \delta/3) D} = e^{-bD} \quad (2)$$

- S_0 – signal intensity without the diffusion weighting.
- S – diffusion-weighted signal.
- γ – gyromagnetic ratio.
- G – amplitude of the two diffusion gradient pulses.
- δ – duration of the pulses.
- Δ – time between the two pulses.
- D – diffusion coefficient is a measure of the strength (velocity) of diffusion in tissue. The stronger the diffusion, the greater the diffusion coefficient, i.e. the ADC in our in vivo case.

The stronger the gradients, the longer they are applied and the more spread out in time, the greater the b-factor.

D. What is the Optimum b-value?

Images obtained with the lowest b-values (0-100 sec/mm²) provide T2-weighted EPI image with lower signal-to-noise ratio for anatomical reference. However, they included external effects due to perfusion or microvascularization.

In the range of clinically relevant b-values (up to approximately 1000), the greater the b-value, the stronger the diffusion weighting and higher the contrast in pathogenic regions is notice.

Higher b-values may depict even more lesions, at the price of poor SNR due to longer TEs and increased susceptibility. Increasing averages, which result in longer scan times, can compensate this [4]. Changing the b-value immediately influences other parameters like minimal TE, slice thickness and FOV as well as maximum matrix at a given optimal bandwidth. Furthermore anisotropy of tissues, also influences the choice (Fig. 4).

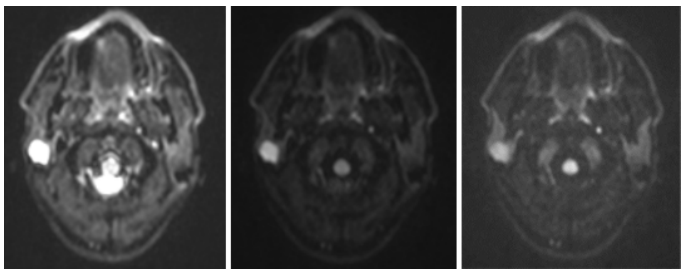

Fig. 4. Values b50 b500 b1000

A. Why do most Head and Neck DWI Protocols Start with b-value 50 s/mm²?

The selection of a low b-value larger than zero provides suppression of large vessels, which makes lesions more conspicuous. The calculation of the tissue ADC can be more accurate when starting with even higher b-values like 100 or 200, to omit the contribution of flow and micro vascular effects.

Low b-values more often serve as anatomical reference. The fact of using b-value 0 in head and neck diffusion is for a shorter period of acquisition or seek greater SNR.

Fig. 4 shows examples of three b-values: b 50, b 500, and b 1000 s/mm².

B. Why is a Minimum of three Directions Measured for each high b-value?

The sensitivity of these sequences is limited to diffusion in the direction of the gradients, so they must be repeated by applying diffusion gradients in at least 3 spatial directions, and diffusion may be different in all three dimensions.

Diffusion magnitude, calculated from the 3 diffusion images thus obtained, minimize the influence of anisotropy, renders the image weighted in global diffusion (trace image). The ADC images are therefore different depending on the sensitizing direction.

The 'trace image' displays the geometric averaging of all three directional measurements, resulting in trace-weighted images. It suppresses to some extent anisotropy information and focuses on differences in signal attenuation. Like the ADC map, the trace-weighted map shows the strength of the diffusion and not its orientation.

Two diffusion sequences with different b-factors can be used to quantitatively measure the degree of molecular mobility, by calculating the ADC, which is represented in the form of a map, whose values (in s/mm²) no longer depend on T2. An ADC hyposignal thus corresponds to a restriction in diffusion.

C. How is the ADC Calculated?

Having measured a set of at least 2 different b-value images (e.g., b 0 and b 1000 s/mm²) the system calculates pixel by pixel the ADC by linear regression.

$$\text{Signal ADC} = -\ln(S/S0)/\ b \qquad (3)$$

The ADC pixel values together form the ADC map. On a half logarithmic scale, the signal decay delivers a straight tilted line whose slope provides the ADC. The faster the signal decay the steeper the slope and the higher the ADC.

The Diffusion image (b 1000) below displays reduced diffusion as hyperintense (brighter pixels); in contrast the ADC map displays it as hypointense (darker pixels).

D. Why should I measure three or more b-values for a DWI protocol when two would be enough for calculating ADC?

While two b-values are sufficient for creating an ADC image, the selection of three b-values (b 50, b 500, b 1000) delivers a more accurate calculation of the ADC values (Fig. 5).

The lower SNR of the b 1000 images introduces a higher standard deviation of the ADC that is partially compensated by the median value of b500.

Here is an example of two ADC images, the first acquired with three b-values and the second with two b-values (Fig. 6).

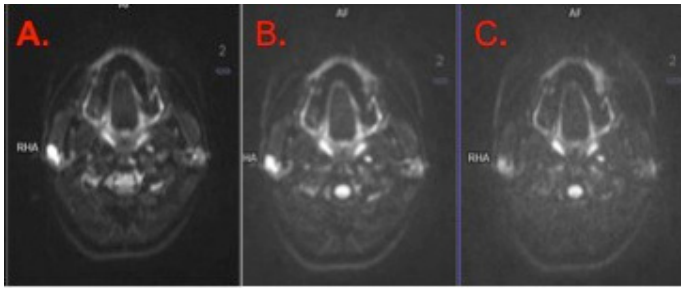

Fig. 5. Values b50 b500 b1000

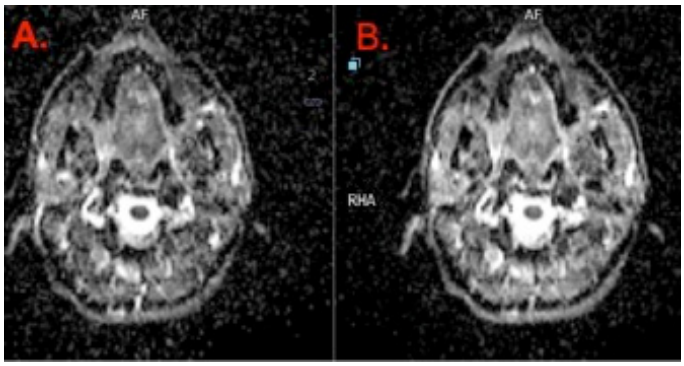

Fig. 6. ADC 3 values de b ADC 2 values b

E. Why do we Need ADC Images, and What does the 'A' in ADC Stand For?

Diffusion sequences are actually T2 weighted sequences, sensitized to diffusion by gradients.

The contrast of the diffusion image will have both diffusion and T2 component, which must be taken into consideration in the interpretation. In areas with long T2, this can simulate reduced diffusion ('T2 Shine-Through' effect). Calculating a pure diffusion coefficient can eliminate these portions of the signal.

The 'A' stands for apparent because we do not measure the pure diffusion coefficient (D or DC). In-vivo tissues, as well as the diffusion processes, have superimposed a capillary pseudo diffusion and gross motion to which the MR measurement is also very sensitive.

F. Why are some Lesions Typically Brighter than the Background Head and Neck Tissue on the Higher b-value Image and Darker on the ADC Map?

Due to the nature of certain lesions and their missing perfusion, the cells swell and hinder a normal diffusion; i.e., the mean free path is shorter. Water molecules cannot move as far in the damaged tissue as in normal tissue [5]. As a result, the ADC is lower and appears darker than the surrounding normal tissue.

G. Which Benefit does the Calculation of an Exponential Map Deliver?

Diffusion imaging cannot distinguish between water molecules motion and different microscopic movements such as those occurring in the microcirculation. Depending on the tissue composition, water molecule movements are different, that is the reason for measuring the apparent diffusion in each voxel.

The exponential map or image is calculated by dividing the maximal b-value diffusion-weighted image by the b0 image. Mathematically the exponential map displays the negative exponential of the ADC; it is a synthetic DW image without T2 'shine-through' effect [6].

The contrast behavior is similar to the high b-value image (Fig. 7).

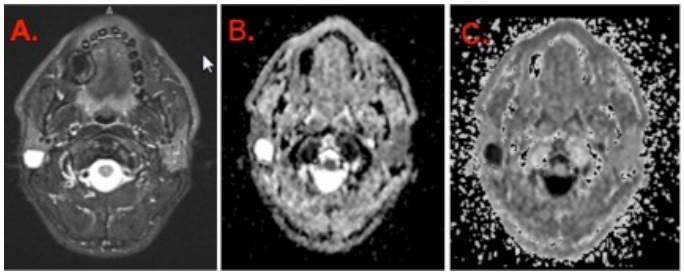

Fig. 7. A. Axial T2 with fat suppression showing a hyperintense lesion in the right parotid gland. B. Notice the high signal intensity of the lesion In the ADC map. C. and the low signal in the exponential map.

H. Why Fat Saturation is Important in Studies of Diffusion?

In most applications the diffusion gradients are integrated in echo planar imaging (EPI) sequences, which exhibit high signal intensity in areas with restricted diffusion as well as in fatty tissue.

Furthermore, the fat signal is displaced in the direction of the chemical shift as compared to the water signal. This makes fat saturation techniques necessary to identify the lesions in the diffusion-weighted images.

There are several techniques to suppress the fat signal in MRI.

For head and neck DWI protocols the fat saturation based on SPAIR technique (SPectral Attenuated Inversion Recovery) is a good compromise between acquisition time, SNR and artifacts homogeneity and STIR (Short Tau Inversion Recovery, another fat saturation technique) provides a more homogeneous fat saturation, free of artifacts.

I. Why DWI in Head and Neck Imaging is so Sensitive to Artifacts?

The most common artifacts are those related with imaging distortion due to the field inhomogeneity and to the differences in magnetic susceptibility from the anatomical tissues that compound this region; besides the presence of air-tissue interfaces, metal implants, dental amalgams or implants common in this area.

Another source of artifacts is related with movements, either voluntary or involuntary, such as breathing or coughing. The collaboration of the patient is mandatory to obtain high quality as well as the short as possible acquisition times.

J. High-resolution DWI, RESOLVE

Single-shot echo-planar imaging (EPI) is well established as the method of choice for clinical, diffusion-weighted imaging with MRI because of its low sensitivity to the motion-induced phase errors that occur during diffusion sensitization of the MR signal.

However, the method is prone to artifacts due to susceptibility changes at tissue interfaces and has a limited spatial resolution.

RESOLVE (multi-shot EPI sequence) is the combination of readout segmented EPI and parallel imaging can be used to address these issues by generating high-resolution, diffusion-weighted images with a significant reduction in susceptibility artifact compared with the single-shot case. The technique uses data from a 2D navigator acquisition to perform a nonlinear phase correction and to control the real-time reacquisition of unusable data that cannot be corrected (Fig. 8).

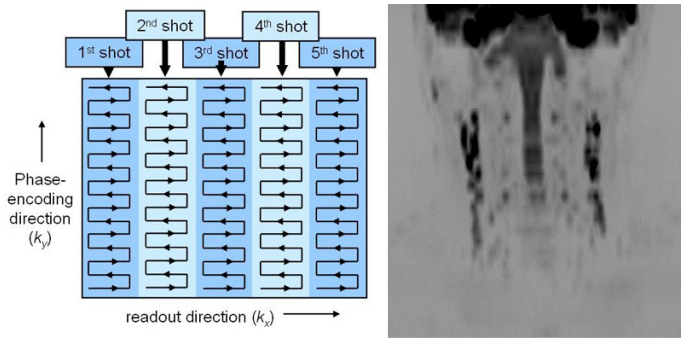

Fig. 8. RESOLVE sequence.

K. Which new DWI Features are Introduced with Software for Siemens?

There is a new 'body diffusion' application card with many new applications [7]:

- diffusion scheme monopolar/bipolar
- start ADC calculation for b > = …
- exponential ADC; no T2 shine-through
- invert gray scale ("PET-like" image) (Fig. 9).
- calculated image of artificial b-values plus (Fig. 9).
- choice of dynamic field correction
- improved fat saturation schemes

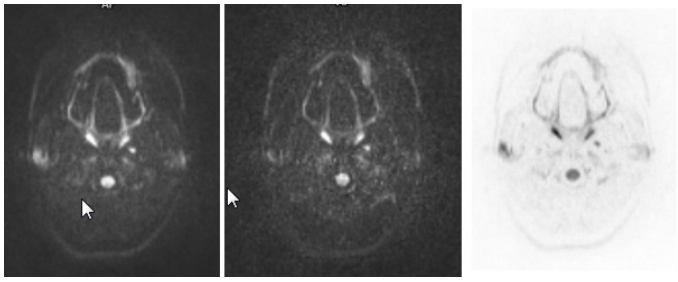

Fig. 9. B1000 Calculated image artificial b1400 Invert gray scale

L. Image Evaluation

DWI analysis is usually qualitative, evaluating the signal intensity of the images obtained with high b-values as well as the correlation with the ADC map. This analysis can also be quantitative calculating the ADC values, placing a ROI (region of interest) on the ADC map sequence and recording the mean value in that ROI. A value of 1000 intensity points is to be interpreted as 1 x 10^{-3} mm^2/s. There are more complex methods such as parametric response maps that allow segmenting a tumor by providing better information about the intratumoral heterogeneity.

I. Clinical Applications

The variation in motion and redistribution of water molecules between tissue compartments that is reflected in DW Imaging and ADC values helps to differentiate disease processes [5] and to characterize tissues, providing complementary information to conventional structural MR imaging [8].

At our institution most of the studies for imaging head and neck pathology are performed in a 1.5 Tesla MR scanner (Avanto Siemens, Erlangen, Germany), using EPI-DW sequences with 3 different b values (0, 500 and 1000 s/mm^2).

It is important not to use a different MR scanner or change the imaging protocol during a patient follow up, as ADC values may differ significantly between MRI systems and sequences. In fact, ADC measurements obtained by one person and in the same MR imaging system, protocol, and sequence are reproducible and independent of time.

In head and neck region, anatomical structures such as the lymph nodes, tonsillar tissue, spinal cord and nerve roots are associated with non-pathological restricted diffusion probably due to their high cellularity or highly packed internal structure [9]. Variable diffusion is usually observed within submandibular and parotid glands. The spinal cord and tonsillar tissue are the structures with the lowest ADC variability and therefore should serve as reference tissue for head and

neck region studies. This is especially relevant evaluating treatment response of a tumor as they can be used for comparison.

DWI in head and neck, mainly in cancer patients, is indicated for tissue characterization of primary tumors and nodal metastases, prediction and monitoring of treatment response after chemotherapy or radiation therapy, and differentiation of radiation changes and residual or recurrent disease [10].

A. Characterization of Primary Tumors

Head and neck cancers account for the sixth most common type of cancer worldwide, causing significant morbidity and mortality, being tobacco and alcohol consumption important risk factors. Differentiation of malignant head and neck tumors from benign lesions and accurate definite diagnosis is essential for treatment planning as well as for prognosis of malignant tumors.

The most relevant reports found that the mean ADC values of benign solid tumors were higher than those observed in malignant tumors, as a result of their histopathological differences.

In general, malignant tumors with hypercellularity, enlarged nuclei, and a reduced extracellular matrix, have a smaller diffusion space of water protons hence reducing ADC values [11]. A threshold ADC value of 1.22 x 10^{-3} mm^2/s provided an accuracy of 86% sensitivity, 84% specificity and 91% for predicting malignancy [12-14].

Furthermore, due to differences in the internal architecture of each lesion, variability in ADC values was reported within each group of tumor (benign or malignant) [12]. (Fig. 10 & 11).

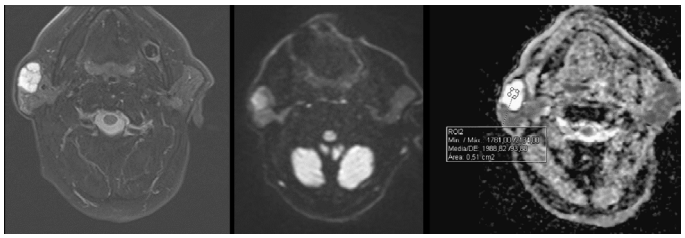

Fig. 10. Benign mixed tumour (BMT) in the superficial lobe of the right parotid gland. A. Axial T2-WI: high-signal round lesion. B. In DW b 1000 is hyperintense. C. On ADC map it does not show restrict diffusion, high signal intensity (1.98 × 10−3 mm^2/sec). The BMT (which contains myxoid tissue) has the highest ADC values of all salivary gland neoplasms, commonly in keeping with benign nature.

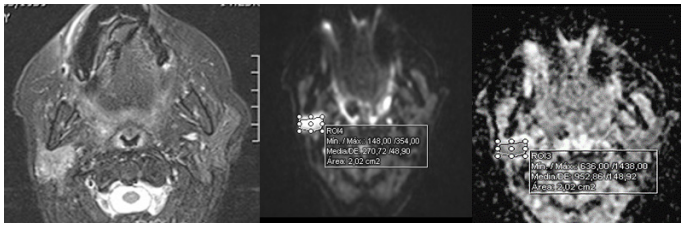

Fig. 11. Malignant tumor of the right parotid gland. A. Axial T2-WI showing a heterogeneous, mostly hyperintense, lesion. B. On DW b1000 is hyperintense. C. On ADC map has low signal intensity (0.952 × 10^{-3} mm2/sec) consistent with restricted diffusion.

In fact, among squamous cell carcinomas (SCC), those showing highly or moderately differentiated histological type present higher ADC values, than poorly differentiated SCC [13-14]. This may be explained by the presence of liquefactive necrosis in the highly differentiated type.

DWI and ADC values can help to discriminate between SCC and non-Hodgkin Lymphoma; pathologic differences between these two tumors, such as the greater cellularity in lymphomas lead to a different behavior in this sequence. Usually lymphomas present greater diffusion restriction and hence lower ADC values [15-16] . The reported mean ADC for lymphoma is fairly consistent, in the range of 0.64 to 0.66 x 10^{-3} mm^2/sec [14, 16]. Distinguishing between SCC and lymphoma is important to optimize the treatment of these patients. Usually SCCs require complex surgeries with extensive resections and reconstructions, alone or combined with radiation therapy and/or chemotherapy, and lymphomas are usually treated with radio-chemotherapy.

Salivary gland tumors are a rare condition, accounting for less than 3% of all head and neck cancers [17]. The salivary gland tumors display a wide spectrum of histologic features tumors are composed of distinctive tissues (tumor cells, myxomatous tissues, lymphoid tissues, necrosis, and cysts). Conventional MRI has limited utility in differentiation of salivary gland tumors [18, 19]; on the other hand DWI is demonstrated to be very sensitive to biophysical abnormalities within the tumor. Preoperative prediction of tumor malignancy is clinically very important, because this information strongly influences the surgical plan. The most common benign salivary gland tumors are pleomorphic adenomas and Warthin tumors. In general, pleomorphic adenomas have highest ADC values due to the cystic or myxomatous component that characterized them, while Warthin tumors have lowest ADC values in keeping with the presence of lymphoid tissue [20] (Fig. 12).

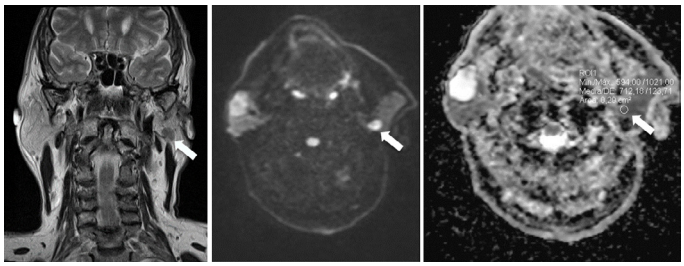

Fig. 12. Warthin tumour (lymphomatous adenoma) in the left parotid gland. A. A smoothly marginated mass, low to intermediate signal in coronal T2-WI MR. B. It is hyperintense on DWI (b 1000 sec/mm^2) (arrow). C. On ADC map it shows low signal intensity (0.71 × 10^{-3} mm^2/sec) (arrow), compatible with restricted diffusion. See the difference with the contralateral tumor in the right parotid gland, which was a benign mixed tumour (BMT).

The ADC maps for malignant salivary gland tumors (such as mucoepidermoid carcinomas) demonstrate relatively homogeneous areas of low ADC values (that represent cell proliferation), in contrast to other salivary gland tumors, for example lymphomas arising in the salivary glands, that are associated to extremely low ADC values (because of the presence of lymphoma cells) [15].

Anyway, in some cases, there is considerable overlap of ADC values, and DWI alone may not be sufficient to discriminate between benign and malignant salivary gland tumors [21, 22].

B. Evaluation of Lymph Nodes

The presence of cervical lymph node metastases is the most important prognostic factor in head and neck squamous cell carcinomas as this worsens the treatment outcome. Pretreatment staging is crucial in the management of head and neck cancer, and it has been considered one of the most important aspects in the selection of treatment options.

Differentiation between inflammatory and metastatic lymphadenopathy is often challenging with conventional imaging [23]. Also, morphologic and size criteria in MRI are not enough for the assessment of lymph node metastases.

DW imaging can help to detect cervical lymph node metastases, and to differentiate between benign and malignant enlarged lymph nodes. The general consensus appears to be that ADCs of malignant lymph nodes are significantly lower than those of normal lymph nodes [13, 23, 24]. Threshold ADC values (1.0-1.38x$10^{-3}$$mm^2$/s) have been reported to differentiate between malignant and benign lymph nodes

[13, 23, 25]. De Bondt et al reported a threshold, when ADC is lower than 1.0×10^{-3} mm²/s this was the strongest independent predictor of presence of metastasis (Fig. 13).

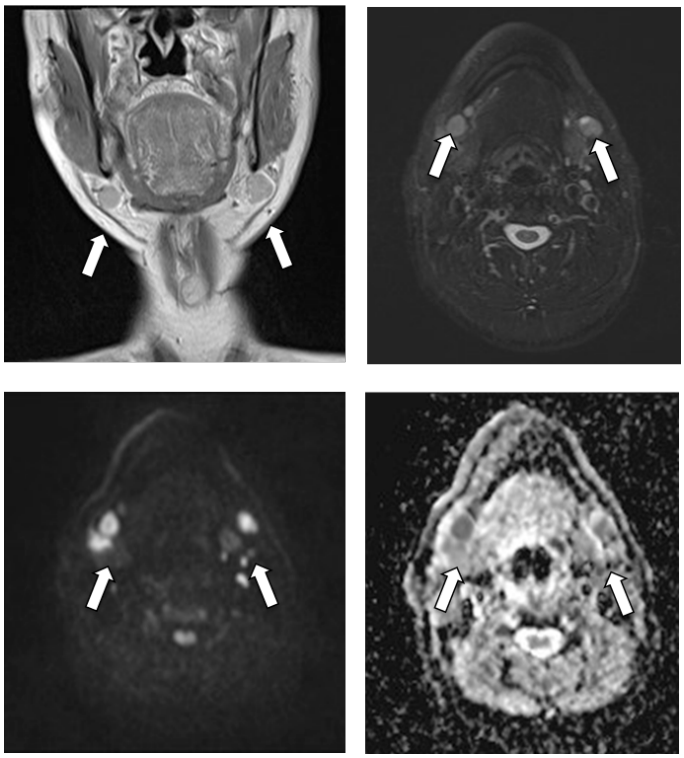

Fig. 13. Metastatic lymph nodes from nasopharyngeal carcinoma. A. Abnormal lymph nodes in bilateral submandibular regions (arrows) show intermediate signal intensity in coronal T1-WI and B. in fat saturations axial T2-WI. C. These nodes are hyperintense on DWI (b value 1000 sec/mm²) (arrows). D. On ADC map they show low signal intensity (from 0.64×10^{-3} mm²/sec to 0.86×10^{-3} mm²/sec) (arrows), compatible with restricted diffusion.

DWI can be better in differentiating between malignant and benign lymph nodes when abnormal lymph nodes show significantly different diffusion characteristics to normal lymph nodes within the same patient, as it is easy to compare. Despite the promising potential of DWI in detection of small malignant lymph nodes, low in-plane resolution of ADC maps and the presence of image artifacts can impact negatively on specificity and reproducibility of findings. For this reason, DWI should always be interpreted in conjunction with other MRI sequences to improve diagnostic accuracy [10]. Nowadays, depicting small metastatic lymph nodes (<4 mm) and lymph nodes with micrometastases that are below the resolution of currently available morphologic MR and DW images, remains challenging.

C. Monitoring and Prediction of Treatment Response after Chemotherapy or Radiation Therapy

The prognosis of patients with SCC of the head and neck remains poor despite aggressive therapeutic regimens and technological advances in surgery [26]. DWI is a noninvasive imaging biomarker to predict tumor response and one of the greatest potential benefits of DW imaging lies in the identification of the group of patients who could respond or fail to respond to therapy. Furthermore this technique could detect disease before clinical signs or symptoms are evident.

As DWI evaluates the motion of water molecules within intracellular and extracellular spaces, it reflects biological changes in tumor microenvironment, and therefore changes in ADC may imply changes in tumor composition.

There are published data that suggest the change in ADC over the course of treatment may indeed be a predictor of outcome [27-29], and could be use in monitoring treatment response. A treatment-induced increase in ADC during therapy for head and neck squamous cell carcinoma has been confirmed in several studies, and results suggest that tumors that show a lower increase or even a decrease in ADC are more likely to fail treatment [24, 28, 30, 31, 32] (Fig. 14 & 15).

Vandencaveye and colleagues reported ADC changes before pretreatment studies and 3 weeks after chemo or radiotherapy allows early assessment of treatment response. This allows early assessment of treatment response. The ADC showed a PPV of 89% and a NPV of 100% for primary lesions and a PPV of 70% and a NPV of 96% for lymph nodes33.

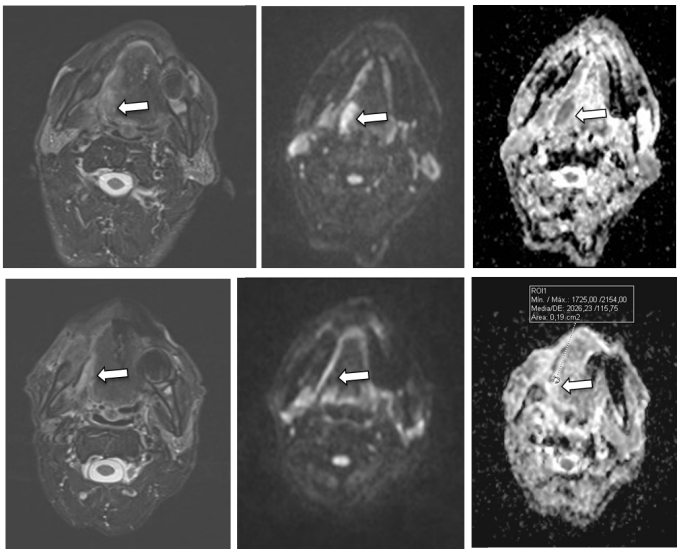

Fig. 14. Oropharyngeal carcinoma. A. A focal area of abnormal signal intensity in the base of the tongue and right tonsil (arrow) in axial T2-WI is seen. B. It is hyperintense onDWI (b value 1000 sec/mm²) (arrow). C. On ADC map it shows low signal intensity (values not shown) (arrow), compatible with restricted diffusion. In this case, the restricted-diffusion lesion most likely corresponds to malignancy.

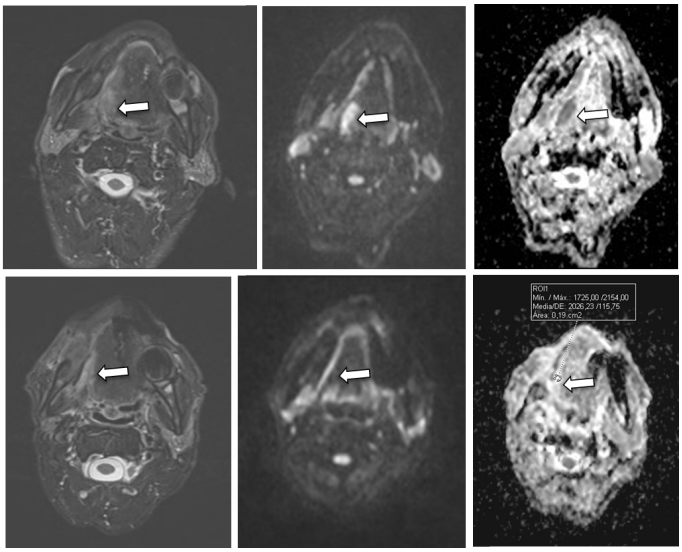

Fig. 15. Oropharyngeal carcinoma. Same patient from Fig. 14, imaging after treatment (chemotherapy and radiation therapy). A. There is a significant decrease in the size of the focal area of abnormal signal intensity in the base of the tongue and right tonsil (arrow) in axial T2-WI. B. This area is no longer hyperintense on DWI B 1000 sec/mm² (arrow). C. On ADC map it shows high signal intensity (2.02×10^{-3} mm²/sec) (arrow), i.e., there is no longer restriction of diffusion. A partial remission (partial response to the treatment) in MRI involves not only morphological improvement (T1-WI, T2-WI) but also complete or partial resolution of restricted diffusion in lesions with this feature.

These findings could lead to stop ineffective treatments and to avoid delays in starting alternative and maybe more effective therapies.

It could also be important to develop prognostic imaging markers that can accurately predict treatment response before therapy. These imaging biomarkers may help in stratifying patients into those who would benefit from chemo-radiation therapy from those who would not. DWI studies of HNSCC have suggested that ADC can be used as a potential marker for prediction of treatment response and long-term survival [28, 32, 34]. These results are consistent with the hypothesis that a high pretreatment ADC value may be indicative of micronecrosis and, consequently, of hypoxia-mediated increased resistance to treatment and poor prognosis in these patients [35].

Kim and cols reported that the mean ADC of responders increases significantly after one week and it increases until the end of treatment. Values were found to be higher in complete responders than in partial responders [30].

This technique potentially could help in the detection of responder or not responder patients.

D. Residual or Recurrent Disease

Chemotherapy or radiation therapy changes and recurrent neck tumor have similar CT and MR appearance and are difficult to differentiate. Anatomical distortion due to surgery and the presence of edema and necrosis after chemo-radiation therapy may difficult the interpretation of the findings [36].

FDG-PET/CT may help to detect recurrent SCC [37], but inflammatory changes within the first 4 months following radiotherapy is an important confounding factor, even biopsies performed after radiotherapy to identify residual/recurrent disease are often equivocal [38].

Qualitative DW imaging analysis after treatment may be helpful and is most of the times is performed by means of visual assessment of signal intensity on DW images [39].

Post-therapeutic changes induced by radio or chemotherapy can be visualized as high, or sometimes also low, signal intensity on high-b-value images but generally show high signal intensity on the corresponding ADC map, as compared with tumors [10].

Recurrent head and neck SCCs are seen as soft-tissue masses with high FDG uptake in PET-CT, moderately high T2 signal intensity, and moderate to high contrast enhancement. At DW imaging, recurrent tumor shows restricted diffusion with low ADCs (most often $<1.3 \times 10^{-3}$ mm^2/sec) [28, 33, 39], which allows differentiation from benign radiation therapy–induced changes (ADC $>1.6–1.8 \times 10^{-3}$ mm^2/sec) [13, 40].

Although ADCs often allow differentiation between tumor and inflammation, reported ADC thresholds differ from one series to another because of variable technical parameters used by various investigators [33, 39, 41]. For example, Vandecaveye et al [33] reported a high sensitivity (94.6%), specificity (95.9%) and accuracy (95.5%) for DWI to distinguish between tumoral and nontumoral tissue. The ΔADC showed a PPV of 89% and an NPV of 100% for primary lesions and a PPV of 70% and an NPV of 96% for lymph nodes. They also found that DWI yielded fewer false positives in comparison with CT or PET for both residual primary tumor and lymph node metastases.

As there may be some overlap between ADCs measured in recurrent tumors and those in radiation therapy–induced inflammatory tissue, DW imaging findings must be correlated with morphologic MR imaging findings.

II. What About the Future?

DWI has been shown to add value in several areas by being part of the multi-parametric MRI approach, even though quantitative values tend to overlap.

Investigations into the clinical applications are still at an early stage. A challenge that DWI faces is standardization of imaging protocols allowing for better comparisons across studies, getting higher spatial resolution for better tumor delineation, to depict smaller lesions, to reduce susceptibility artifacts and acquisition times.

The improvement of other (nonEPI) techniques, less sensitive to artifacts, such as halfFourier single-shot turbo spin-echo (HASTE), the split acquisition of fast spin-echo signals (SPLICE), PROLLELER, or BLADE could lead into a better approach to this difficult area. To achieve field homogeneity, both 1.5 Tesla and 3 Tesla, allowing better fat suppression could also be helpful.

There are new applications in this field: diffusion scheme monopolar/bipolar, start ADC calculation for b >, exponential ADC; no T2 shine-through, invert gray scale (“PET-like” image) calculated image of artificial b-values plus, choice of dynamic field correction, improved fat saturation scheme.

Moreover, to develop methods to analyze ADC maps more accurately will be essential as well as the standardization of the technique acquisition and post processing methods that would allow setting thresholds and integrating them in clinical settings.

Finally, it will be crucial to correlate DWI with morphology on MRI and other functional techniques, such as Perfusion MRI, Dynamic Contrast Enhanced (DCE) Imaging and PET to reach a better clinical approach.

References

[1] Ozgen B, Oguz KK, Cila A. Diffusion MR Imaging Features of Skull Base Osteomyelitis Compared with Skull Base Malignancy. Am J Neuroradiol [Internet]. 2011 Jan 1;32 (1):179–84. Available from: http://www.ajnr.org/content/32/1/179.abstract

[2] Le Bihan D, Breton E, Lallemand D, Grenier P, Cabanis E, Laval-Jeantet M. MR imaging of intravoxel incoherent motions: application to diffusion and perfusion in neurologic disorders. Radiology. UNITED STATES; 1986 Nov;161(2):401–7.

[3] Stejskal EO, Tanner JE. Spin Diffusion Measurements: Spin Echoes in the Presence of a Time Dependent Field Gradient. J Chem Phys. 1965;42(1).

[4] Kingsley PB, Monahan WG. Selection of the optimum b factor for diffusion-weighted magnetic resonance imaging assessment of ischemic stroke. Magn Reson Med. United States; 2004 May;51(5):996–1001.

[5] Padhani AR, Liu G, Koh DM, Chenevert TL, Thoeny HC, Takahara T, et al. Diffusion-weighted magnetic resonance imaging as a cancer biomarker: consensus and recommendations. Neoplasia. Canada; 2009 Feb;11(2):102–25.

[6] Provenzale JM, Engelter ST, Petrella JR, Smith JS, MacFall JR. Use of MR exponential diffusion-weighted images to eradicate T2 “shine-through” effect. Am J Roentgenol [Internet]. American Roentgen Ray Society; 1999 Feb 1;172(2):537–9. Available from: http://dx.doi.org/10.2214/ajr.172.2.9930819

[7] Hagmann P, Jonasson L, Maeder P, Thiran J-P, Wedeen VJ, Meuli R. Understanding diffusion MR imaging techniques: from scalar diffusion-weighted imaging to diffusion tensor imaging and beyond. RadioGraphics. United States; 2006 Oct;26 Suppl 1:S205–23.

[8] Schafer J, Srinivasan A, Mukherji S. Diffusion magnetic resonance imaging in the head and neck. Magn Reson Imaging Clin N Am. United States; 2011 Feb;19(1):55–67.

[9] Kolff-Gart AS, Pouwels PJW, Noij DP, Ljumanovic R, Vandecaveye V, de Keyzer F, et al. Diffusion-Weighted Imaging of the Head and Neck in Healthy Subjects: Reproducibility of ADC Values in Different MRI Systems and Repeat Sessions. Am J Neuroradiol [Internet]. 2015 Feb 1;36 (2):384–90. Available from: http://www.ajnr.org/content/36/2/384.abstract

[10] Thoeny HC, Keyzer F De, King AD. Diffusion-weighted MR Imaging in the Head and Neck 1. Radiology. 2012;263(1):19–32.

[11] Guo AC, Cummings TJ, Dash RC, Provenzale JM. Lymphomas and high-grade astrocytomas: comparison of water diffusibility and histologic characteristics. Radiology. United States; 2002 Jul;224(1):177–83.

[12] Srinivasan A, Dvorak R, Perni K, Rohrer S, Mukherji SK. Differentiation of Benign and Malignant Pathology in the Head and Neck Using 3T Apparent Diffusion Coefficient Values: Early Experience. Am J Neuroradiol [Internet]. 2008 Jan 1;29 (1):40–4. Available from: http://www.ajnr.org/content/29/1/40.abstract

[13] Abdel Razek AAK, Soliman NY, Elkhamary S, Alsharaway MK, Tawfik A. Role of diffusion-weighted MR imaging in cervical lymphadenopathy. Eur Radiol. Germany; 2006 Jul;16(7):1468–77.

[14] Wang J, Takashima S, Takayama F, Kawakami S, Saito A, Matsushita T, et al. Head and neck lesions: characterization with diffusion-weighted echo-planar MR imaging. Radiology. United States; 2001 Sep;220(3):621–30.

[15] Sumi M, Ichikawa Y, Nakamura T. Diagnostic ability of apparent diffusion coefficients for lymphomas and carcinomas in the pharynx. Eur Radiol. Germany; 2007 Oct;17(10):2631–7.

[16] Maeda M, Kato H, Sakuma H, Maier SE, Takeda K. Usefulness of the apparent diffusion coefficient in line scan diffusion-weighted imaging for distinguishing between squamous cell carcinomas and malignant lymphomas of the head and neck. AJNR Am J Neuroradiol. United States; 2005 May;26(5):1186–92.

[17] Harnsberger, H.R., Wiggins, R.H., Hudgins, P.A., Michel, M.A., Swartz, J., Davidson HC et al. Diagnostic imaging: head and neck. Salt Lake City, UT; Amirsys; 2004.

[18] Freling NJ, Molenaar WM, Vermey A, Mooyaart EL, Panders AK, Annyas AA, et al. Malignant parotid tumors: clinical use of MR imaging and histologic correlation. Radiology. UNITED STATES; 1992 Dec;185(3):691–6.

[19] Joe VQ, Westesson PL. Tumors of the parotid gland: MR imaging characteristics of various histologic types. AJR Am J Roentgenol. UNITED STATES; 1994 Aug;163(2):433–8.

[20] Eida S, Sumi M, Sakihama N, Takahashi H, Nakamura T. Apparent diffusion coefficient mapping of salivary gland tumors: prediction of the benignancy and malignancy. AJNR Am J Neuroradiol. United States; 2007 Jan;28(1):116–21.

[21] Matsushima N, Maeda M, Takamura M, Takeda K. Apparent diffusion coefficients of benign and malignant salivary gland tumors. Comparison to histopathological findings. J Neuroradiol. France; 2007 Jul;34(3):183–9.

[22] Habermann CR, Arndt C, Graessner J, Diestel L, Petersen KU, Reitmeier F, et al. Diffusion-weighted echo-planar MR imaging of primary parotid gland tumors: is a prediction of different histologic subtypes possible? AJNR Am J Neuroradiol. United States; 2009 Mar;30(3):591–6.

[23] de Bondt RBJ, Nelemans PJ, Hofman PAM, Casselman JW, Kremer B, van Engelshoven JMA, et al. Detection of lymph node metastases in head and neck cancer: a meta-analysis comparing US, USgFNAC, CT and MR imaging. Eur J Radiol. Ireland; 2007 Nov;64(2):266–72.

[24] Galbán CJ, Mukherji SK, Chenevert TL, Meyer CR, Hamstra DA, Bland PH, et al. A Feasibility Study of Parametric Response Map Analysis of Diffusion-Weighted Magnetic Resonance Imaging Scans of Head and Neck Cancer Patients for Providing Early Detection of Therapeutic Efficacy. Transl Oncol [Internet]. Neoplasia Press Inc.; 2009 Aug 18;2(3):184-90. Available from: http://www.ncbi.nlm.nih.gov/pmc/articles/PMC2730136/

[25] Vandecaveye V, De Keyzer F, Vander Poorten V, Dirix P, Verbeken E, Nuyts S, et al. Head and neck squamous cell carcinoma: value of diffusion-weighted MR imaging for nodal staging. Radiology. United States; 2009 Apr;251(1):134–46.

[26] Zorat PL, Paccagnella A, Cavaniglia G, Loreggian L, Gava A, Mione CA, et al. Randomized phase III trial of neoadjuvant chemotherapy in head and neck cancer: 10-year follow-up. J Natl Cancer Inst. United States; 2004 Nov;96(22):1714–7.

[27] Hatakenaka M, Nakamura K, Yabuuchi H, Shioyama Y, Matsuo Y, Ohnishi K, et al. Pretreatment apparent diffusion coefficient of the primary lesion correlates with local failure in head-and-neck cancer treated with chemoradiotherapy or radiotherapy. Int J Radiat Oncol Biol Phys. United States; 2011 Oct;81(2):339–45.

[28] King AD, Mo FKF, Yu K-H, Yeung DKW, Zhou H, Bhatia KS, et al. Squamous cell carcinoma of the head and neck: diffusion-weighted MR imaging for prediction and monitoring of treatment response. Eur Radiol. Germany; 2010 Sep;20(9):2213–20.

[29] Hamstra DA, Lee KC, Moffat BA, Chenevert TL, Rehemtulla A, Ross BD. Diffusion magnetic resonance imaging: an imaging treatment response biomarker to chemoradiotherapy in a mouse model of squamous cell cancer of the head and neck. Transl Oncol. United States; 2008 Dec;1(4):187–94.

[30] Kim S, Loevner L, Quon H, Sherman E, Weinstein G, Kilger A, et al. Diffusion-weighted magnetic resonance imaging for predicting and detecting early response to chemoradiation therapy of squamous cell carcinomas of the head and neck. Clin Cancer Res. United States; 2009 Feb;15(3):986–94.

[31] Berrak S, Chawla S, Kim S, Quon H, Sherman E, Loevner LA, et al. Diffusion weighted imaging in predicting progression free survival in patients with squamous cell carcinomas of the head and neck treated with induction chemotherapy. Acad Radiol. United States; 2011 Oct;18(10):1225–32.

[32] Vandecaveye V, Dirix P, De Keyzer F, de Beeck KO, Vander Poorten V, Roebben I, et al. Predictive value of diffusion-weighted magnetic resonance imaging during chemoradiotherapy for head and neck squamous cell carcinoma. Eur Radiol. Germany; 2010 Jul;20(7):1703–14.

[33] Vandecaveye V, Dirix P, De Keyzer F, Op de Beeck K, Vander Poorten V, Hauben E, et al. Diffusion-weighted magnetic resonance imaging early after chemoradiotherapy to monitor treatment response in head-and-neck squamous cell carcinoma. Int J Radiat Oncol Biol Phys. United States; 2012 Mar;82(3):1098–107.

[34] Whitcher B, Schmid VJ, Collins DJ, Orton MR, Koh D-M, Diaz de Corcuera I, et al. A Bayesian hierarchical model for DCE-MRI to evaluate treatment response in a phase II study in advanced squamous cell carcinoma of the head and neck. MAGMA. Germany; 2011 Apr;24(2):85–96.

[35] Chawla S, Kim S, Dougherty L, Wang S, Loevner LA, Quon H, et al. Pretreatment Diffusion-Weighted and Dynamic Contrast-Enhanced MRI for Prediction of Local Treatment Response in Squamous Cell Carcinomas of the Head and Neck. Am J Roentgenol [Internet]. American Roentgen Ray Society; 2013 Jan 1;200(1):35–43. Available from: http://dx.doi.org/10.2214/AJR.12.9432

[36] Tartaglino LM, Rao VM, Markiewicz DA. Imaging of radiation changes in the head and neck. Semin Roentgenol. UNITED STATES; 1994 Jan;29(1):81–91.

[37] Terhaard CH, Bongers V, van Rijk PP, Hordijk GJ. F-18-fluoro-deoxy-glucose positron-emission tomography scanning in detection of local recurrence after radiotherapy for laryngeal/ pharyngeal cancer. Head Neck. United States; 2001 Nov;23(11):933–41.

[38] Bar-Ad V, Mishra M, Ohri N, Intenzo C. Positron Emission Tomography for Neck Evaluation Following Definitive Treatment with Chemoradiotherapy for Locoregionally Advanced Head and Neck Squamous Cell Carcinoma. Rev Recent Clin Trials [Internet]. 2012 Feb;7(1):36–41. Available from: http://www.ncbi.nlm.nih.gov/pmc/articles/PMC3809074/

[39] Varoquaux A, Rager O, Dulguerov P, Burkhardt K, Ailianou A, Becker M. Diffusion-weighted and PET/MR Imaging after Radiation Therapy for Malignant Head and Neck Tumors. RadioGraphics [Internet]. Radiological Society of North America; 2015 Aug 7;35(5):1502–27. Available from: http://dx.doi.org/10.1148/rg.2015140029

[40] Tshering Vogel DW, Zbaeren P, Geretschlaeger A, Vermathen P, De Keyzer F, Thoeny HC. Diffusion-weighted MR imaging including bi-exponential fitting for the detection of recurrent or residual tumour after (chemo) radiotherapy for laryngeal and hypopharyngeal cancers. Eur Radiol. Germany; 2013 Feb;23(2):562–9.

[41] Sadick M, Schoenberg SO, Hoermann K, Sadick H. Current oncologic concepts and emerging techniques for imaging of head and neck squamous cell cancer. GMS Curr Top Otorhinolaryngol Head Neck Surg. Germany; 2012;11:Doc08.

Cristina Utrilla Contreras

Cristina Utrilla Contreras is neuroradiologist in University Hospital La Paz, in Madrid, Spain. After finishing the studies in Complutense University in Madrid in 2006, she completed the residency program in Radiology in University Hospital La Paz in 2011. She participated in the European School of Radiology Exchange Programme for Neuroradiology Fellowship during 2013 in University Hospital Freiburg. She has published several papers in international journals and presented communications in national and international meetings. Doctor Utrilla presented her PhD work entitled: “The value of volumetric computed tomography in the study of the Chronic Obstructive Pulmonary Disease” in April 2016.

Begoña Marin Aguilera

Graduate of Medicine and Surgery in 2001. Medical specialist in Radiology in 2007. Neuroradiology specialist in La Paz University Hospital (from May 2008 to present) with training and experience to perform Vascular and Interventional Neuroradiology. Author of several publications in the field of specialization and collaborator in investigation projects. Participation as speaker in courses of medical specialization. Tutor specialty (2011-2015).

Nelson Mauricio Buitrago Sánchez

Radiology and Internal Medicine specialist. Currently practicing in the neuroradiology area, La Paz University Hospital, Madrid (Spain).

Joachim Graessner

Siemens Healthcare GmbH
Collaboration Management MR
HC CEMEA GER SV ES&DS CM
Lindenplatz 2
20099 Hamburg, Deutschland

Pilar García Raya

Neuroradiologist since 1993 to present in University Hospital La Paz, Madrid, Spain. Residency in Radiology in La Paz University Hospital 1989-1992. Graduate/ Medical School in Madrid Autonoma University 1982-1988. Membership of Spanish Society of Neuroradiology and European Society of Neuroradiology. Member of La Paz University Hospital Head and Neck Cancer multidisciplinary Committee with several collaborations in specialiced meetings and courses.